NeuroImage 186 (2019) 70–82

Contents lists available at ScienceDirect

NeuroImage

journal homepage: www.elsevier.com/locate/neuroimage

Dynamic low frequency EEG phase synchronization patterns during proactive control of task switching

María Eugenia López [a,b,c,**,1], Sandra Pusil [b,d,1], Ernesto Pereda [b,e], Fernando Maestú [a,b,c], Francisco Barceló [d,*]

[a] Department of Experimental Psychology, Psychological Processes and Speech Therapy, Universidad Complutense of Madrid, Spain
[b] Laboratory of Cognitive and Computational Neuroscience (UCM-UPM), Centre for Biomedical Technology (CTB), Madrid, Spain
[c] Networking Research Center on Bioengineering, Biomaterials and Nanomedicine (CIBER-BBN), Madrid, Spain
[d] Laboratory of Neuropsychology, University of the Balearic Islands, Spain
[e] Electrical Engineering and Bioengineering Group, Department of Industrial Engineering & IUNE, Universidad de La Laguna, Tenerife, Spain

ARTICLE INFO

Keywords:
Electroencephalogram
Proactive control
Switch task
Inter-trial phase coherence
Behavioral accuracy
Functional networks

ABSTRACT

Cognitive flexibility is critical for humans living in complex societies with ever-growing multitasking demands. Yet the low-frequency neural dynamics of distinct task-specific and domain-general mechanisms sub-serving mental flexibility are still ill-defined. Here we estimated phase electroencephalogram synchronization by using inter-trial phase coherence (ITPC) at the source space while twenty six young participants were intermittently cued to switch or repeat their perceptual categorization rule of Gabor gratings varying in color and thickness (switch task). Therefore, the aim of this study was to examine whether a proactive control is associated with connectivity only in the frontoparietal theta network, or also involves distinct neural connectivity within the delta band, as distinct neural signatures while preparing to switch or repeat a task set, respectively. To this end, we focused the analysis on late-latencies (from 500 to 800 msec post-cue onset), since they are known to be associated with top-down cognitive control processes. We confirmed that proactive control during a task switch was associated with frontoparietal theta connectivity. But importantly, we also found a distinct role of delta band oscillatory synchronization in proactive control, engaging more posterior frontotemporal regions as opposed to frontoparietal theta connectivity. Additionally, we built a regression model by using the ITPC results in delta and theta bands as predictors, and the behavioral accuracy in the switch task as the criterion, obtaining significant results for both frequency bands. All these findings support the existence of distinct proactive cognitive control processes related to functionally distinct though highly complementary theta and delta frontoparietal and temporoparietal oscillatory networks at late-latency temporal scales.

1. Introduction

Daily activities normally occur in multi-task environments. Even habitual and well-learned behaviors such as driving a car or writing a letter typically involve some type of cognitive control to manage multiple chunks of sensorimotor information chronologically and hierarchically organized towards certain goal that we commonly refer to as “tasks”. Successful performance in such situations needs not only a careful selection and maintenance of the final task's goal, but also of each sub-goal and its corresponding stimulus-response (S-R) mappings, so as to flexibly update the correct S-R mappings proactively whenever contextual cues anticipate a change in the task goals or sub-goals (Grange and Houghton, 2014). Therefore, proactive cognitive control demands a flexible adjustment to newly relevant S-R mappings for efficient execution of upcoming actions to guide goal-directed behavior in changing environments (Cooper et al., 2015). In this way, humans can effectively prepare for a change in task goals or sub-goals even in anticipation of the imperative target stimulus that is to be overtly responded to. For accomplishing this, it is required to regulate interactions between distant brain regions to produce effective, purposeful goal-directed behavior

* Corresponding author. Laboratory of Neuropsychology, University of the Balearic Islands (UIB), 07122, Palma de Mallorca, Balearic Islands, Spain.
** Corresponding author. Department of Experimental Psychology, Psychological Processes and Speech Therapy, Universidad Complutense of Madrid (UCM), 28223, Pozuelo de Alarcón, Madrid, Spain.
E-mail addresses: meugenia.lopez@ctb.upm.es (M.E. López), f.barcelo@uib.es (F. Barceló).
[1] These authors contributed equally to this work.

https://doi.org/10.1016/j.neuroimage.2018.10.068
Received 14 April 2018; Received in revised form 4 October 2018; Accepted 26 October 2018
Available online 28 October 2018
1053-8119/© 2018 Elsevier Inc. All rights reserved.

(Yeung, 2006).

For decades researchers have studied cognitive control using variants of the task-switching paradigm (Kiesel et al., 2010; Rogers and Monsell, 1995; Vandierendonck and Liefooghe, 2010). The cued task-switching paradigm is well suited for studying proactive control and related top-down processes (Corbetta and Shulman, 2002). This paradigm implicates a contextually relevant sensory stimulus (cue) that informs participants what overt response is to be executed upon the onset of the behaviorally relevant (target) stimulus. The task cues may or may not explicitly announce the correct S-R mapping to be used next (Kiesel et al., 2010). However, cognitive demands are maximally engaged when using transition cues, which implicitly prompt to switch ('switch cue') or repeat ('repeat cue') to a newly correct S-R mapping. Thus, transition cues are valuable because they can give us information about the neural substrates implicated in the proactive control of the currently active perception-action rule.

However, there is still a debate about the neural mechanisms directly involved in cognitive control, top-down processes and task switching paradigms. Proactive control has been related with the activation of the lateral prefrontal cortex (Braver, 2012; Dreher and Berman, 2002; Zanto et al., 2011) while parietal regions have been usually associated with attentional control (Le et al., 1998; Toth and Assad, 2002). These two regions have been postulated to be part of a so-called 'fronto-parietal network' or 'cognitive control network' responsible for accomplishing a wide panoply of executive functions involved in goal-directed behavior (Cole et al., 2013; Corbetta and Shulman, 2002; Vincent et al., 2008).

In recent years, results from task-based functional magnetic resonance imaging (fMRI) have argued for an extension of the model of cognitive control beyond the frontal and parietal cortices. Several studies have suggested the existence of large-scale brain systems involved in cognitive control such as top-down attentional control, task-set maintenance, implementation, inhibition, and trial by trial control (Dosenbach et al., 2008; Power and Petersen, 2013). In fact, an influential model of cognitive control defines two anatomically and functionally segregated brain systems that might be central to supporting cognitive control functions; namely, the frontoparietal and cingulo-opercular cortical networks (Cocchi et al., 2013). Most neurophysiological studies to date (using electroencephalography, EEG, and magnetoencephalography, MEG) have found that cognitive control is associated with low oscillatory synchronization activity, and more specifically, theta band (4–8 Hz) oscillations (Cooper et al., 2015; Raghavachari et al., 2006). Moreover, it has been considered a unique role of theta activation promoting the integration of information and enabling goal-directed control processes (Sauseng et al., 2010). On the other hand, the literature also suggests a distinct role of lower frequency oscillations in cued task switching, as several studies found an increase in delta activity related to the execution of cognitive tasks and in cognitively demanding situations (Cooper et al., 2016; Gulbinaite et al., 2014; Harmony et al., 1996).

The study of temporal dynamics, source reconstruction and functional connectivity (FC) provide detailed information about how brain regions coordinate to support higher cognitive functions (Bola and Sabel, 2015; Simpson et al., 2011; Sporns et al., 2004; Wang et al., 2010; Zanto et al., 2011). Thus, this type of analysis offers an insight into the interactions and relationships among different brain regions. In this way, recent task switching EEG and MEG studies have found an implication of slow waves by using functional connectivity analyses (Cavanagh et al., 2009; Cooper et al., 2015; Gladwin et al., 2006; Mansfield and Karayanidis, 2012; Sauseng et al., 2007).

The present work was designed to explore the neural substrates behind the cued task-switching paradigm using EEG functional connectivity measured with phase locking value (PLV) in source space. We compared the temporal dynamics triggered by switch and repeat cues within low frequency EEG oscillations (delta and theta bands) of the whole brain network focusing on a late-latency time window (500–800 msec post-cue onset) when top-down switch-specific control processes are known to maximally engage the fronto-parietal cortical network (Barceló and Cooper, 2018; Cole and Schneider, 2007; Cooper et al., 2015; Zanto et al., 2010) in a sample of 26 healthy young subjects. To our knowledge, there are no studies exploring the whole brain network using functional connectivity analysis in EEG source space using cued task-switching paradigms. We hypothesized a differential involvement of both the fronto-parietal and cingulo-opercular networks in response to either type of cue, with larger large-scale functional connectivity expected for switch compared to repeat cues (Cocchi et al., 2013; Dosenbach et al., 2008). Our findings partly confirmed our original hypotheses about: a) an anticipatory increase of connectivity in both the delta and theta frequency bands, that is expected to be larger in response to switch as compared to repeat cues, presumably due to the larger cognitive demands under switch conditions; and 2) a functionally distinct involvement of the delta and theta bands in either task condition (Braver et al., 2003; Cocchi et al., 2013; Cooper et al., 2015; Dosenbach et al., 2008; Shi et al., 2014; Vincent et al., 2008; Yeung, 2006).

2. Materials and methods

2.1. Participants

Twenty six young adults who were students at the University of the Balearic Islands (2 male, ages = 19–33 years, mean = 22.2 years, SD = 3.67 years) took part in the study (this is a subset of the 31 participants previously used to examine switch-related late ERP positivities by Barceló and Cooper, 2018; see the *EEG analyses* section for details). All of them reported no history of neurological or psychiatric disorders, and presented normal or corrected-to -normal vision. Informed consent was obtained from all participants and experimental procedures and behavioral testing were performed in accordance with the Declaration of Helsinki, and with the approval of the Ethics committee of the university. All participants had an overall hit rate better than 85% in the switch task; with a minimum of 60% trial runs with correct responses to the first three target trials (see Stimuli and Procedures). These strict behavioral criteria ensured that only participants who had understood and complied with task instructions entered the final sample.

2.2. Neuropsychological indexes of cognitive control

A battery of neuropsychological tests was administered that encompassed several indexes of working memory span (Forward and Backward Digit Span, Wechsler Adult Intelligence Scale WAIS-IV (Wechsler, 2008), control of interference (Stroop test; Jensen and Rohwer, 1966), verbal fluency (Controlled Oral Word Association Test – COWAT; Benton and Hamsher, 1976), and as a paper-and-pencil measure of cognitive flexibility, the Madrid card sorting test (MCST), a task-switching analogue of the Wisconsin card sorting test (Adrover-Roig and Barceló, 2010; Barceló, 2003). Task administration was paper-and-pencil except for the

Table 1
Demographic and cognitive scores of 26 young adults. Stroop CW= Stroop Color-Word; Stroop INT= Stroop Interference; Forward DS = Forward Digit Span; Backward DS = Backward Digit Span; COWAT= Controlled Oral Word Association Test; Efficient MCST series = Number of efficient series in a modified version of the Wisconsin Card Sorting Test (MCST); Perseverative MCST series = Number of series containing perseverative errors in the MCST.

Variables	Mean	Standard Deviation
Age	22.2	3.67
Stroop CW	49.4	7.34
Stroop INT	5.2	5.97
Forward DS	9.9	1.56
Backward DS	8.0	1.78
COWAT	39.7	8.41
Efficient MCST series	9.8	1.24
Perseverative MCST series	0.5	0.65
Accuracy Switch task (% correct)	90.0	0.02

computerized cued task-switching procedure as described below. Table 1 summarizes the descriptive statistics of the selected neuropsychological indexes for our sample of young participants.

2.3. Stimuli and procedures

Participants sat in an electrically shielded, sound attenuated, and dimly lit room at a viewing distance of 150 cm from a 27-inch video LCD monitor (800 × 600 at 75 Hz), with a response pad in their hands. Stimuli consisted of four equally probable ($p = 0.21$), colored Gabor patches with horizontally oriented gratings (either red or blue, 4 or 10 cpd, 25% contrast, 1° visual angle, 3.5 cd/m^2), and two infrequent ($p = 0.08$) gray Gabor patches (oriented either vertically or horizontally, 2 cpd, 25% contrast, 1° visual angle, 3.5 cd/m^2), displayed against a gray background (2.85 cd/m^2) at a visual angle of 6.5° to the left or to the right of a central fixation cross with 0.5° × 0.5° of visual angle. The central fixation cross remained continuously present throughout the experiment.

The experiment consisted of a switch task, which involved different motor responses depending on the cue stimuli (switch or repeat) (Fig. 1). A 972-trial sequence was semi-randomly generated offline, with the constraint that trial runs between two consecutive gray Gabor patches contained a varying number of four to eight colored patches. This trial sequence was divided into six blocks to allow for short self-paced breaks every 5 min, approximately. On each trial, a Gabor patch appeared for 100 msec on the left or right visual hemifields, and participants had a maximum of 1200 msec to respond with a button press on designated target trials. Both response speed and accuracy were emphasized in the instructions prior to each task. Wrong or late responses, as well as false alarms (i.e., button presses to non-target gray gratings) were followed by feedback to help subjects keep track of the correct rule. As a consequence, stimulus onset asynchrony (SOA) was either 1900 or 2400 msec on correct and incorrect trials respectively (i.e., depending on feedback presentation). However, since trial runs containing any kind of errors were disregarded from the analyses, SOA was 1900 msec for all trials examined in this study. Tasks were administered in counterbalanced order between participants to control for learning effects.

All participants were presented with exactly the same trial sequence during the experiment. Before the switch task, a short block of 74 test trials was administered to warrant that task instructions had been understood. Stimuli display and behavioral response collection were carried out using Presentation® software (Neurobehavioral Systems Inc., Albany, CA). The switch task was a variant of the intermittent-instruction paradigm (Monsell, 2003; Rushworth et al., 2002). Participants were instructed to fixate their gaze on the central cross and to sort the colored Gabor patches according to two classification rules, either the color or thickness of the gratings (i.e. spatial frequency) by pressing a key with their left or right index fingers. When sorting by the color rule, subjects pressed the right button for 'red' and the left button for 'blue'. When sorting by thickness, subjects used the right key for 'thin' and the left key for 'thick'. The horizontal and vertical gray gratings instructed subjects to either 'repeat' or 'switch' the previous rule. The relation between gray grating orientation and instruction was counterbalanced between participants (Fig. 1).

2.4. Electrophysiological recordings

Continuous EEG data (0.05–100 Hz bandpass) were collected using SynAmps RT amplifiers (NeuroScan, TX, USA) from 60 scalp sites using tin electrodes mounted on an elastic cap (Synamp2 Quikcap, Compumedics, TX) at a sampling rate of 500 Hz. EEG electrodes were placed following the extended 10–20 position system (Fp1, Fp2, AF7, AF3, AFz, AF4, AF8, F7, F5, F3, F1, Fz, F2, F4, F6, F8, FT7, FC5, FC3, FC1, FCz, FC2, FC4, FC6, FT8, T7, C5, C3, C1, Cz, C2, C4, C6, T8, TP7, CP5, CP3, CP1, CPz, CP2, CP4, CP6, TP8, P7, P5, P3, P1, Pz, P2, P4, P6, P8, PO7, PO3, POz, PO4, PO8, O1, Oz, O2) and were referenced to the left mastoid. The electrodes were later re-referenced offline to the average reference. Four additional electrodes were placed above and below the left eye and on the outer canthi of both eyes to monitor blinks and eye movements. Sensor impedances were kept below 10 kΩ.

2.5. Behavioral analyses

At the beginning of the Switch task, subjects were instructed to begin sorting by color up to the onset of the first gray grating in the trial run. These trials were eliminated from the analyses. Reaction times (RTs) were analyzed from correct trial runs only, and those trial runs containing any false alarm, omission, or any other errors were discarded. Error trials were used to compute accuracy indexes. Only the first and third target responses in a trial run (after a gray grating) were considered for behavioral analysis, since behavioral costs in intermittently instructed paradigms typically reach an asymptote in later trials (Monsell, 2003; Rushworth et al., 2002).

2.6. EEG analyses

Only trials accepted for behavioral analyses entered the cue-locked EEG analyses, whereas trial runs containing errors, false alarms and omissions were discarded in both tasks. EEG data were epoched into

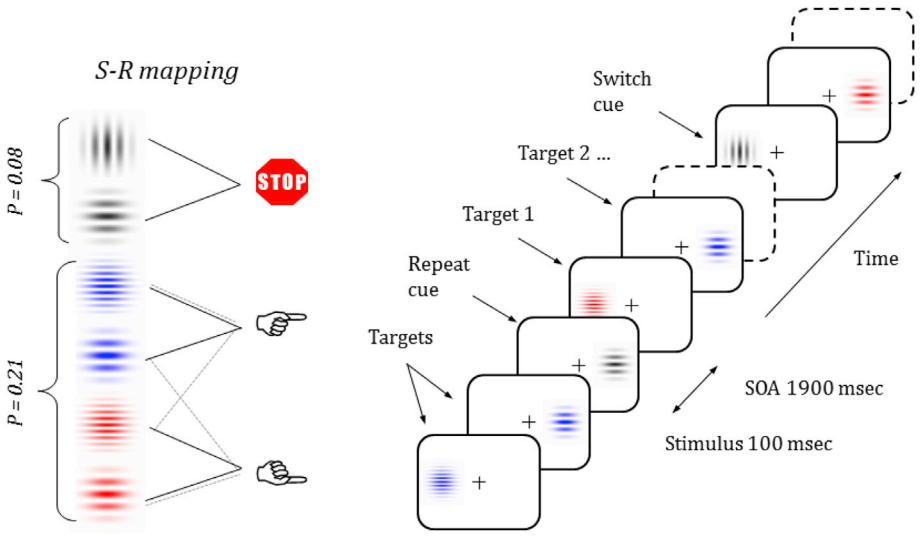

Fig. 1. Task design, stimulus material, and stimulus-response (S–R) mappings. In this Switch task, vertical and horizontal gray gratings instructed participants to switch or repeat the previous S-R mapping, respectively. Participants were explicitly instructed not to respond to the gray Gabor patches. Hypothetical task-set information and S-R mappings for correct performance are also shown for the task. Task demands were manipulated by varying the amount of contextual information conveyed by the gray gratings for anticipatory updating of active S-R mappings (see Methods section).

segments of 1700 msec (from −500 to 1200 msec relative to cue onset), and were merged together for each task condition and participant. Epochs containing non-stereotyped artifacts (e.g., cable movement, swallowing), and residual artifacts larger than ± 100 μV were manually removed by visual inspection based on their scalp topographies, time courses, and activation spectra using Brainstorm (Tadel et al., 2011). A maximum of two bad channels per subject were detected by visual inspection and excluded from processing. Those epochs containing stereotyped artifacts (e.g., eye blinks, muscle artifact, etc.) were retained. Independent Component Analysis (ICA-Infomax; EEGLAB) (Bell and Sejnowski, 1995) was applied to each task condition in order to isolate stereotyped artifacts (e.g., eye blinks, muscle artifact, etc.). A maximum of 4 components were removed for each subject and condition. Then, EEG data were reconstructed without those components. Subsequently, signals were extended at both sides (mirror padding) to avoid edge effects and then, they were band-pass filtered in the traditional frequency ranges, namely delta (2–4 Hz), theta (4–8 Hz), alpha (8–12 Hz), beta (12–30 Hz) and gamma (30–46 Hz). In the present work, we focused on the slow frequency range (delta and theta bands) which is assumed to underlie proactive control of task switching (Cooper et al., 2015; Sauseng et al., 2010).

At least 55 trials per condition and participant after artifact rejection were used for further analysis (range 55–65 trials across participants). The mean number of trials that entered the EEG analyses did not differ significantly between switch and repeat conditions. This dataset was partly the same to that used to examine late frontoparietal ERP positivities in task switching (Barceló and Cooper, 2018). Therefore, from the original subset of 31 participants examined in that previous study, only 26 subjects with a minimum of 55 clean trials per task condition entered in the connectivity analyses. These strict data requirements motivated the exclusion of 5 participants from the original dataset. The final dataset is available online in this web site: https://github.com/LCCN/Neuroimage2018.

2.7. Source reconstruction

Source reconstruction analysis was carried out using the Brainstorm software (Tadel et al., 2011). To this end, we employed the default anatomy included in this toolbox, which consisted of the segmented cortical surface (15,000 vertices) of the MNI/Colin27 brain. A realistic head model of 3 layers (scalp, outer and inner skull) was calculated using the symmetric boundary element method OpenMEEG BEM (Gramfort et al., 2010). To estimate the noise level in the recordings, a noise covariance matrix was computed using the pre-stimulation baseline. Then, to solve the inverse problem, sources were determined with weighted Minimum Norm Estimation (wMNE) (Mosher et al., 2003). wMNE is well-suited for the estimation of large-scale functional connectivity networks, since it addresses the problem of volume conduction, reducing spurious signal correlations (Hassan et al., 2014; Palva and Palva, 2012). The cortex surface was divided into 68 regions of interest (ROI) based on Brainstorm atlas Desikan-Killiany (Desikan et al., 2006), as shown in Table 2. Regions were translated to the Talairach atlas and Brodmann areas in order to establish a resemblance with the task switching literature. The time series of each ROI was extracted by taking the average of all the signals coming from the dipoles of that region.

2.8. Functional connectivity

To study functional connectivity, inter-trial phase coherence (ITPC) was calculated according to Lachaux et al. (1999). ITPC measures the grade of similarity of the relative phase between two signals over many repetitions, and provides an estimation of the degree of synchrony between the signals as a function of time. This method is based on first filtering the signal and then converting it into a complex valued one, from which the corresponding phase is then obtained. The phase $\theta_i\ (t)$ of the filtered signal $x_i(t)$ was obtained using the Hilbert transform:

Table 2
Abbreviations of the 68 regions of interest based on the Brainstorm atlas Desikan-Killiany, and their corresponding translation to the Talairach atlas and Brodmann brain areas.

Abbreviation	Desikan-Killiany Regions	Translation to Talairach and Broadmann areas
ACCc	Caudal Anterior Cingulate	Limbic Lobe, Cingulate Gyrus,24
ACCr	Rostral Anterior Cingulate	Limbic Lobe, Anterior Cingulate, 32
CAL	Pericalcarine	Occipital Lobe, Cuneus, 17
CUN	Cuneus	Occipital Lobe, Cuneus, 18
EC	Entorhinal Cortex	Limbic Lobe, Entorhinal Cortex, 28
FFG	Fusiform Gyrus	Fusiform Gyrus, 20
HES	Transversetemporal	Temporal Lobe, Superior Temporal Gyrus,41&42
IFGop	Parsopercularis	Frontal Lobe, Inferior Frontal Gyrus, 44
IFGorb	Parsorbitalis	Frontal Lobe, Inferior Frontal Gyrus, 47
IFGtri	Parstriangularis	Frontal Lobe, Inferior Frontal Gyrus, 45
INS	Insula	Sub-lobar, Insula, 13
IPL	Inferior Parietal Lobule	Inferior Parietal Lobule, 39
ITG	Inferior Temporal Gyrus	Temporal Lobe, Inferior Temporal Gyrus, 20
LING	Lingual Gyrus	Occipital Lobe, Lingual Gyrus, 18
MCG	Posterior Cingulate Gyrus	Limbic Lobe, Cingulate Gyrus, 24
MFGc	Caudal Middle Frontal Gyrus	Frontal Lobe, Middle Frontal Gyrus, 6
MFGr	Rostral Middle Frontal Gyrus	Frontal Lobe, Middle Frontal Gyrus, 10
MOG	Lateral Occipital Gyrus	Occipital Lobe, Middle Occipital Gyrus, 18
MTG	Middle Temporal Gyrus	Temporal Lobe, Middle Temporal Gyrus, 21
MTGb	Bankssts	Temporal Lobe, Middle Temporal Gyrus, 22
OrbG	Lateral Orbito Frontal Gyrus	Frontal Lobe, Orbital Gyrus, 11
OrbG	Medial Orbito Frontal Gyrus	Frontal Lobe, Orbital Gyrus, 11
PCG	IsthmusCingulate Gyrus	Limbic Lobe, Posterior Cingulate, 31
PCL	Paracentral Lobule	Frontal Lobe, Paracentral Lobule, 6
PCUN	Precuneus	Parietal Lobe, Precuneus, 7
PHG	Parahippocampal	Limbic Lobe, Parahippocampal Gyrus, 36
PoCG	Postcentral Gyrus	Parietal Lobe, Postcentral Gyrus, 1
PreCG	Precentral Gyrus	Frontal Lobe, Precentral Gyrus, 4
SFG	Frontal Pole	Frontal Lobe, Superior Frontal Gyrus, 10
SFG	Superior Frontal Gyrus	Frontal Lobe, Superior Frontal Gyrus, 8
SMG	Supramarginal Gyrus	Parietal Lobe, Supramarginal Gyrus, 40
SPL	Superior Parietal Lobule	Parietal Lobe, Superior Parietal Lobule, 7
STG	Superior Temporal Gyrus	Temporal Lobe, Superior Temporal Gyrus, 22
TPO	Temporal Pole	Temporal Lobe, Superior Temporal Gyrus, 38

$$z_i\ (t) = x_i\ (t) + i \cdot Hilbert\ (x_i\ (t)) = A_i(t) \cdot e^{i\theta_i\ (t)}$$

We used a sliding window of 10 msec size (5 samples) to obtain a series of phases, where $\theta_i^j(n)$, n = 5*Ntrials is the length of the series, $i = 1,..,68$ indicates the reconstructed ROI, and $j = 1,..,N_w$ stands for the number of windows. Then, for each of these concatenated phase series, we calculated the relative phases between every two reconstructed cortical sources $\varphi_{i,k}^j(t) = \theta_i^j(t) - \theta_k^j(t)$ and from these relative phases, we finally estimated the ITPC between two sources as follows:

$$ITPC_{i,k}(j) = \left| < e^{i\varphi_{i,k}^j(t)} > \right| \quad (1)$$

where $< >$ and $| |$ indicate average and absolute value, respectively, and $j = 1,..,N_w$ (see Fig. 2a). Defined in this way, $ITPC_{i,k}(j)$ ranges from 0 (no synchrony) and 1 (perfect phase synchrony) between sources i and k for

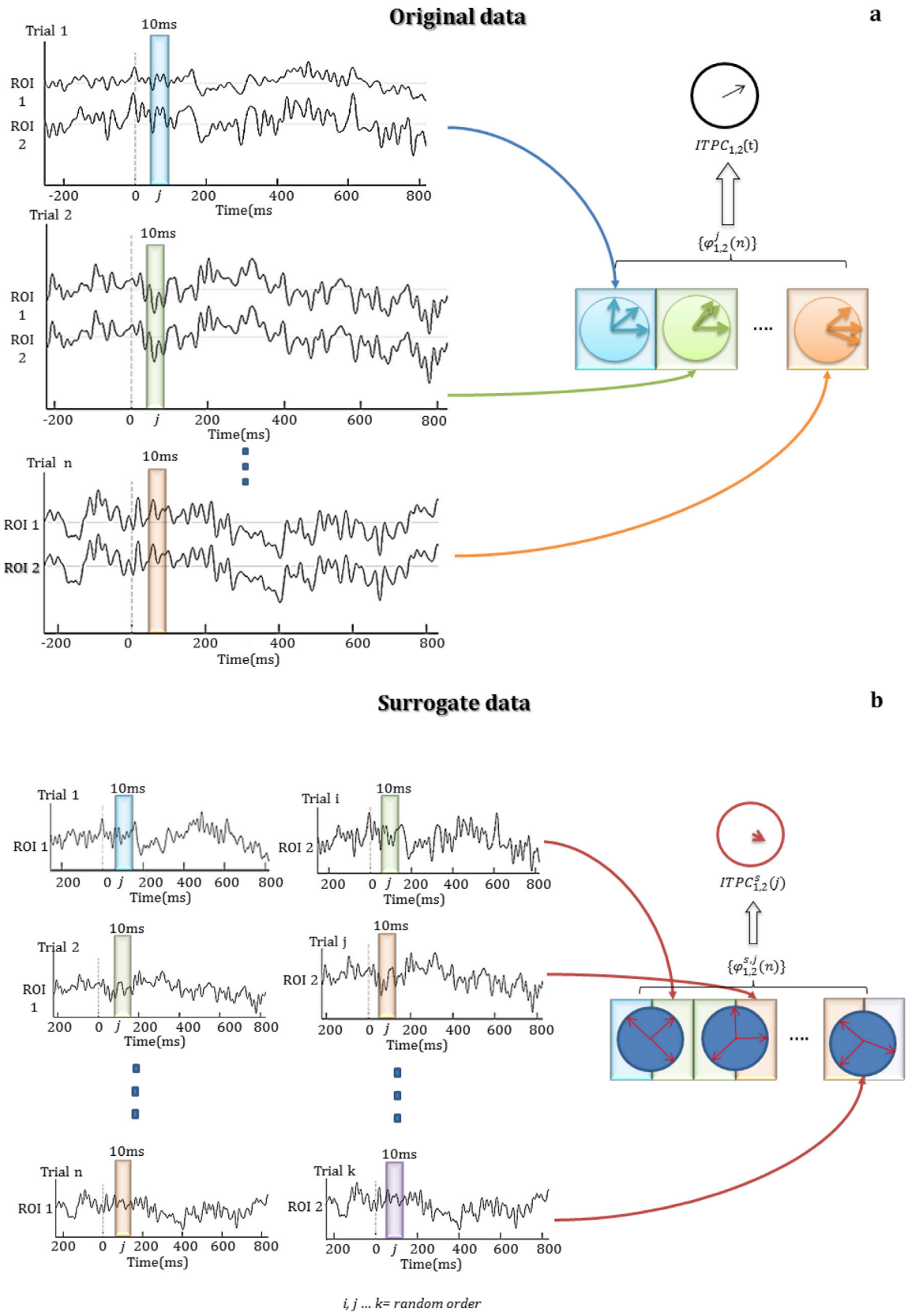

Fig. 2. Inter-trial phase coherence analysis. **(A)** Series of phases are calculated from the filtered signal by using a sliding window of 10 msec for each trial. Then, for each of these concatenated phase series, the relative phases are calculated between every two reconstructed cortical sources $\{\varphi^{j}_{1,2}(n)\}$, and finally the phase locking value is computed. **(B)** Surrogate data is reconstructed by randomly shuffling the order of the trials. Then inter-trial phase coherence analysis is applied as mentioned in Fig. 2a.

window *j*. It provides an estimation of the dynamics of functional connectivity for each pair of sources as a function of time, with a time resolution of 10 msec.

To test the statistical significance of the values of (1) for each subject and channel pair, we used a procedure consisting of randomly shuffling the order of the trials, thereby obtaining different surrogates versions of it, $\varphi^{s,j}_{i,k}(t)$ (s = 1,..,99), where the phase synchrony, if any, between the original signals was removed by construction due to the shuffling procedure. From these shuffled relative phases, we got shuffled $ITPC^{s}_{i,k}(j)$ (see Fig. 2b). The original $ITPC_{i,k}(j)$ is considered as significant, with $p < 0.01$ level of statistical confidence, if it is greater than $ITPC^{s}_{i,k}(j)\ \forall s = 1,..,99$ (non-parametrical significance test). Otherwise, it is set to zero. This test of significance allows removing the spurious ITPC, where the value of the index was not due to actual functional connectivity between two ROIs, but was instead a result of some other feature of the individual signals. In our data, after applying this procedure, a 15% of the original ITPC values were considered not significant.

2.9. Statistical analyses

To further reduce the high dimensionality of the data, and to explore functional connectivity of the well-known Late Positive Component (LPC, 500–800 msec) of the event-related potential (ERP) observed in response to cues in task-switching procedures (see Fig. 3), we selected three time windows of interest each of 100 msec of duration: 500–600 msec, 600–700 msec, and 700–800 msec (Barceló and Cooper, 2018). A decomposition of the total EEG power time-locked to the task cues revealed that task differences in this late latency window largely captured non-phase locked power effects (see Supplementary material). This is a relevant aspect of our analyses as much as the LPC and other endogenous ERP components associated with cognitive control have been related to non-phased locked (induced, or latency variable) EEG activity (Brydges and Barceló, 2018; Cohen and Donner, 2013). Then, a Wilcoxon signed-rank test (nonparametric test for two populations when the observations are paired) was used to compare between conditions (switch vs. repeat) for each frequency band and time window using Matlab v16a. Specifically, for each window, we obtained the average value of the ITPC across the 10 ms windows. Then, we singled out those 100 ms windows/frequency band pairs showing significant differences and tested them using non-parametric permutation test (Maris and Oostenveld, 2007) by pooling the ITPC values on both conditions and randomly dividing them in two equal sets whose size is the number of subjects. A total of 10,000 of such permutations were used for each significant link, and the differences were considered significant with a non-parametric *p value* < 0.001 (after False discovery rate (FDR) corrected for multiple comparison) (Yekutieli and Benjamini, 2001). Finally, we applied stepwise regression analyses using the differences between switch and repeat cues of the significant functional connectivity links obtained in each (delta and theta) band as predictors, and the behavioral accuracy in the switch task as the criterion. Hence, for these regression analyses we employed as dependent variables the values of the connectivity differences, and the overall accuracy (percent correct responses) in the switch task as the criterion. Here we adopted overall task-switching accuracy as the most valid and reliable index of efficient task-switching behavior in line with previous studies using the same task-switching paradigm (Barceló and Cooper, 2018; Cooper et al., 2016).

3. Results

We analyzed functional connectivity differences using ITPC between switch and repeat cues in the delta and theta frequency bands in three time windows (from 500 to 600 msec, from 600 to 700 msec, and from 700 to 800 msec post-cue onset) during the performance of a switch task, obtaining the following results:

3.1. ITPC results

Most of the time windows selected showed greater synchronization values in both delta and theta bands in response to switch compared to repeat cues. Fig. 4 shows the significant links obtained in the functional connectivity analysis ($p < 0.001$, corrected) when comparing switch and repeat cues in delta band (2–4 Hz) in three of the selected time windows (from 500 to 800 msec). Similar results were observed for the theta band (4–8 Hz) when comparing switch and repeat cues (see Fig. 5). Additionally, to exhibit the consistency of effects of the PLV through subjects, Fig. 6 shows the distribution of PLV in critical connections across the 26 subjects with their respective p value.

For the delta band, from 500 to 600 msec post-cue onset (Fig. 4A, D), connectivity values were higher in response to switch compared to repeat cues mostly across right hemisphere regions, thus between Right Inferior Frontal Gyrus (opercular) and Right Supramarginal, Right Paracentral

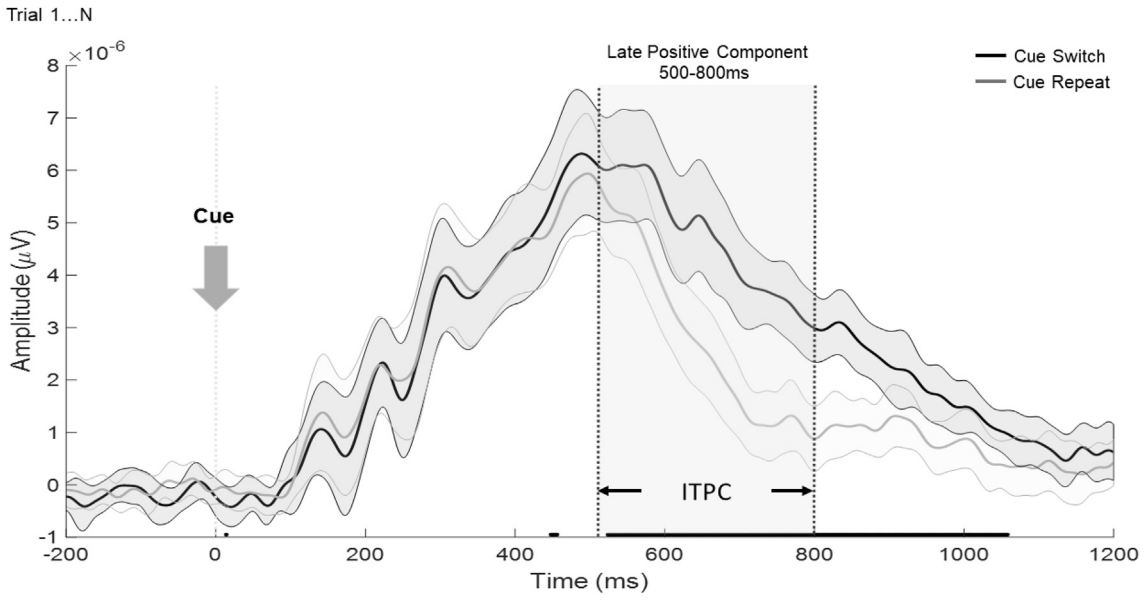

Fig. 3. Timing of the PLV analysis relative to the cue onset. Grand mean ERPs elicited by switch and repeat cues are plotted together with their 95% confidence intervals. The black dots along the x-axis mark time points at which there is a significant paired *t*-test ($P < 0.05$). Code to plot the figure from Rousselet et al. (2016).

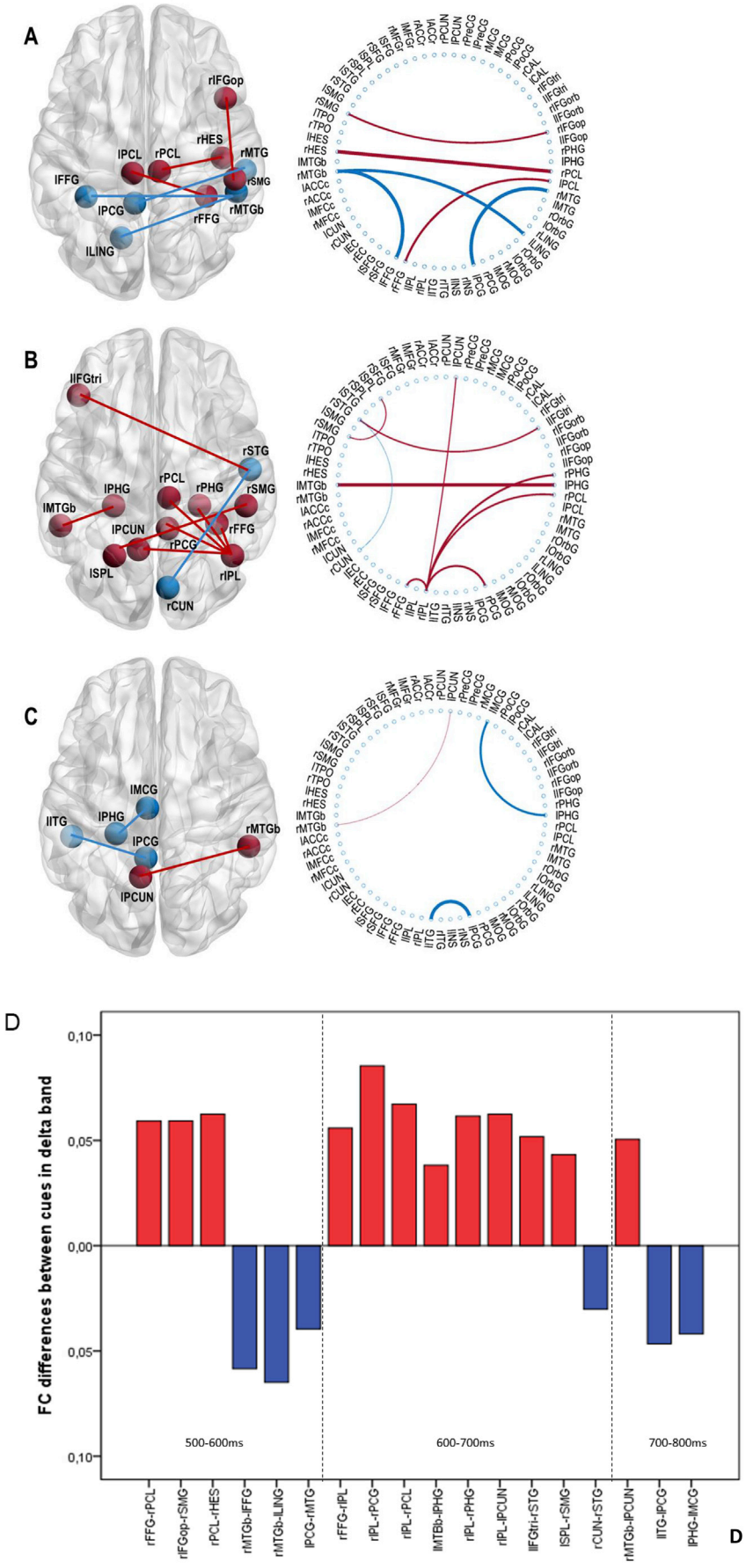

Fig. 4. Significant functional connectivity results ($p < 0.001$, corrected) in the delta band (2–4 Hz) at three time windows: 500–600 msec **(A)**; 600–700 msec **(B)**; and 700–800 msec **(C)** post-cue onset. Red color represents higher connectivity values for switch compared to repeat cues, and blue color illustrates lower connectivity values for switch compared to repeat cues. Additionally, in the circular representation, line thickness of significant links is proportional to ITPC values (a higher value corresponds to thicker lines, and vice versa). **(D)** Functional connectivity differences between switch and repeat cues. Red color indicates greater connectivity following switch cues, and blue color indicates the opposite pattern.

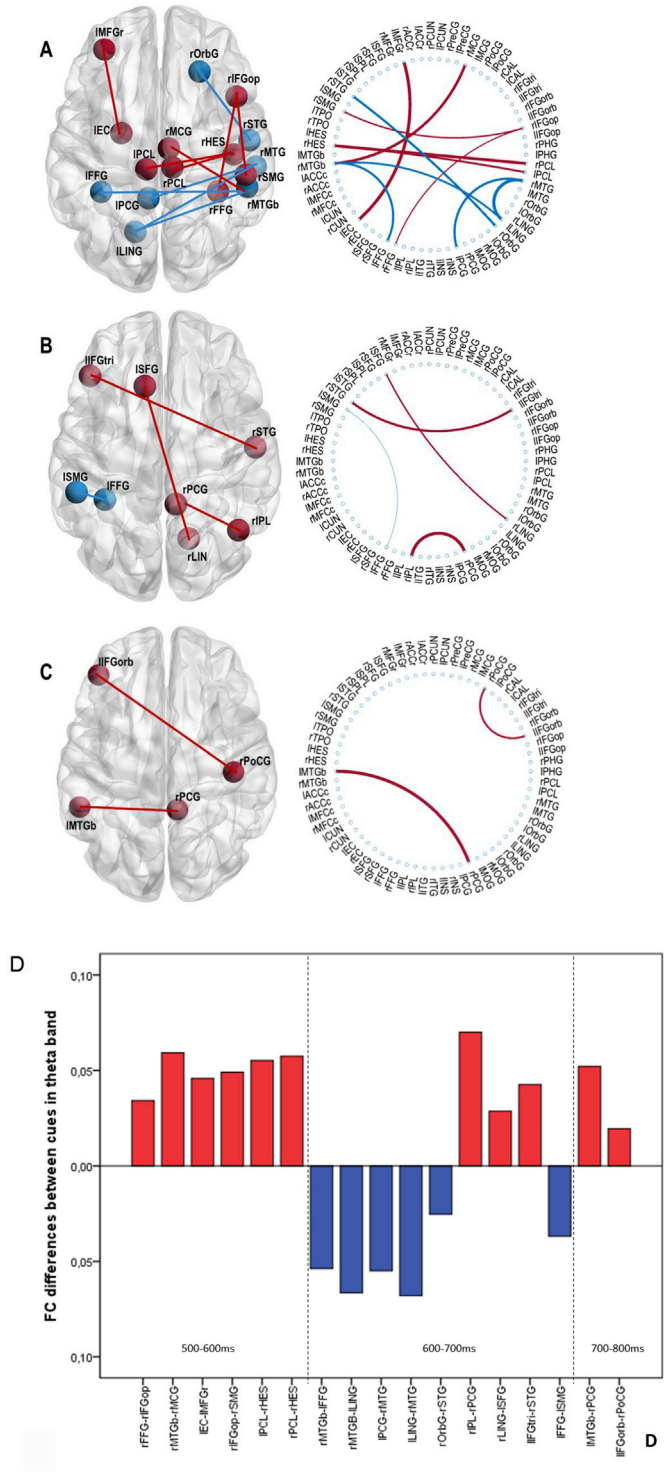

Fig. 5. Significant functional connectivity results ($p < 0.001$, corrected) in the theta band (4–8 Hz) at three time windows: 500–600 msec **(A)**; 600–700 msec **(B)**; and 700–800 msec **(C)** post-cue onset. Red color represents higher connectivity values for switch compared to repeat cues, and blue color illustrates lower connectivity values for switch compared to repeat cues. Additionally, in the circular representation, line thickness of significant links is proportional to ITPC values (a higher value corresponds to thicker lines, and vice versa). **(D)** Functional connectivity differences between switch and repeat cues. Red color indicates a greater connectivity following switch cues, and blue color indicates the opposite pattern.

and Right Superior Temporal Gyrus, as well as between Right Fusiform and Left Paracentral. Moreover, lower connectivity values in response to switch compared to repeat cues were found between Right Middle Temporal Gyrus and Left Fusiform and Left Lingual, Left Posterior Cingulate and Right Middle Temporal Gyrus. For this window and as an illustrative example Fig. 6 shows the distribution of PLV in strong connections across the 26 subjects.

From 600 to 700 msec post-cue onset (Fig. 4B, D), there was an increase of connectivity values in response to switch compared to repeat cues between the Right Inferior Parietal Lobule and several brain regions such as the Right Fusiform, Right Posterior Cingulate, Right Paracentral, Right Parahippocampal, and the Left Precuneus region. Also, switch-related increases in connectivity were found between the Left Middle Temporal Gyrus and the Left Parahippocampal Gyrus, the Left Inferior Frontal Gyrus (triangular) and the Right Superior Temporal Gyrus, and between the Left Superior Parietal and Right Supramarginal gyri, but also a decrease between the Right Cuneus and Right Middle Temporal regions.

Finally, from 700 to 800 msec post-cue onset (Fig. 4C and D), we found higher connectivity values in response to switch compared to repeat cues between the Left Precuneus and the Right Middle Temporal Gyrus, and lower connectivity values between Left Inferior Temporal and Left Posterior Cingulate, and Left Parahippocampal and Left Cingulate Gyrus in response to switch compared to repeat cues.

For the theta band (Fig. 5), we mostly found increased synchronization in response to the switch cue when compared to the repeat cue in the whole time-window explored, namely from 500 to 800 msec post-cue onset. From 500 to 600 msec post-cue (Fig. 5A,D) we found higher connectivity values in Right Fusiform and Right Inferior Frontal Gyrus (opercular), Right Middle Temporal Gyrus and Right Cingulate Gyrus, Left Entorhinal Cortex and Left Middle Frontal, Right Inferior Frontal Gyrus (opercular) and Right Supramarginal and Right Superior Temporal Gyrus and Left/Right Paracentral and lower connectivity values between Right Middle Temporal Gyrus and Left Fusiform and Left Lingual, Right Middle Temporal and Left Posterior Cingulate and Left Lingual, and finally in Right Orbital Gyrus and Right Superior Temporal Gyrus. Additionally, from 600 to 700 msec (Fig. 5B, D), in comparison to the repeat cue, we found an increase in connectivity in the switch cue between the Right Inferior Parietal and the Posterior Cingulate Cortex, the Right Lingual and Superior Frontal Gyrus, and the Left Superior Temporal and the Left Inferior Frontal (triangular) and a decrease in connectivity in the Left Fusiform and the Left Supramarginal. Finally, from 700 to 800 msec, we obtained increased synchronization in response to the switch cue in the Left Middle Temporal Gyrus and Right Posterior Cingulate and Left Inferior Frontal Gyrus (orbital) and Right Postcentral Gyrus (Fig. 5C and D).

3.2. Stepwise regression results

With the aim to explore to what extent the accuracy achieved during the performance of the switch task was explained by the significant ITPC results, we applied a stepwise regression analysis using values of the connectivity differences between switch and repeat trials as dependent variables (Figs. 3D and 4D), and the percent correct responses in the switch task as the criterion. Table 3 presents the final stepwise regression model for the delta band, which revealed two connectivity links (i.e., right paracentral – right superior temporal gyrus, Beta = −0.121, p = 0.007 for model 1; and Beta = −0.152, p = 0.001 for model 2; and left inferior temporal gyrus – left posterior cingulate gyrus, Beta = 0.154, p = 0.036 for model 2) that jointly explained over 34% of variability in behavioral accuracy. Table 4 presents regression results for the theta band, which revealed two connectivity links (i.e., left paracentral – right superior temporal gyrus, Beta = −0.140, p = 0.012 for model 1; and Beta = −0.179, p = 0.002 for model 2; and right orbital gyrus – right superior temporal gyrus, Beta = −0.175, p = 0.035 for model 2) that jointly explained around 32% of variability in behavioral accuracy.

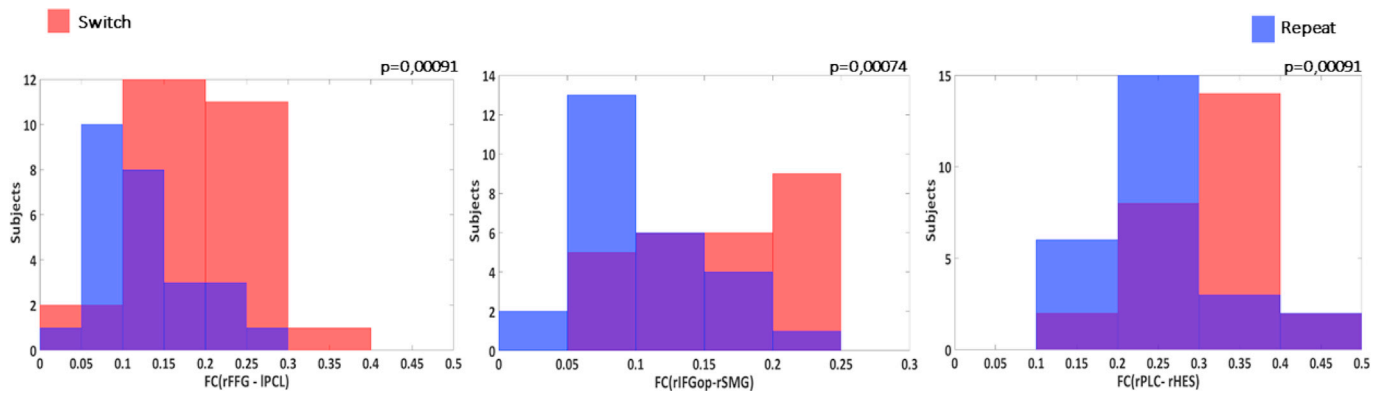

Fig. 6. Illustrative example of the distribution of ITPC values across all subjects in both conditions (blue: repeat, red: switch) for the areas indicated in the x-axis.

Table 3
Results of the stepwise regression analysis for the delta band.

Model	Variables	Beta	R^2 adjusted	Standard Error of the Estimate	F	Sig
1	rPCL - rHES (Fig. 4A)	−0.121	0.235	0.017	8.674	0.007
2	rPCL - rHES lITG - lPCG (Fig. 4C)	−0.152 0.154	0.343	0.016	7.537	0.001 0.036

Table 4
Results of the stepwise regression analysis for the theta band.

Model	Variables	Beta	R^2 adjusted	Standard Error of the Estimate	F	Sig
1	lPCL - rHES (Fig. 5A)	−0.140	0.206	0.017	7.484	0.012
2	lPCL - rHES rOrbG - rSTG (Fig. 5A)	−0.179 −0.175	0.321	0.016	6.898	0.002 0.035

Interestingly, for both delta and theta bands, larger PCL – rHES connectivity values in repeat compared to switch trials were predictive of better performance (Fig. 7).

4. Discussion

The present study used cortical EEG functional connectivity to identify synchronized brain cortical regions involved in a switching paradigm in a sample of 26 healthy young subjects. To this end, we analyzed the connectivity brain patterns in slow frequency bands (delta and theta) during late-latencies (from 500 to 800 msec) post-cue onset, known to be associated with top-down cognitive control processes. The current findings showed that compared to a repeat cue, the response to a switch cue showed an increase in functional connectivity in both delta and theta bands in most of the time windows studied. In general, this increment in functional connectivity may be interpreted as the need to coordinate and use more brain resources to attend cognitively demanding stimuli and to proactively control and flexibly adjust to newly relevant S-R mappings for efficient execution of upcoming actions.

In the delta band, we found an increase in connectivity 500–600 msec post-cue between right pars opercularis and right supramarginal gyrus for the switch cue in comparison with the repeat cue. Both brain areas are part of the fronto-parietal network, which is involved in top-down processes in task-switching (Cocchi et al., 2013; Mansfield and Karayanidis, 2012). Besides, recent studies suggest that the connectivity between fronto-parietal regions may reflect the voluntary orientation of attention toward unexpected and task-relevant stimuli (Harper et al., 2017). Additionally, these two regions have been related to task preparation

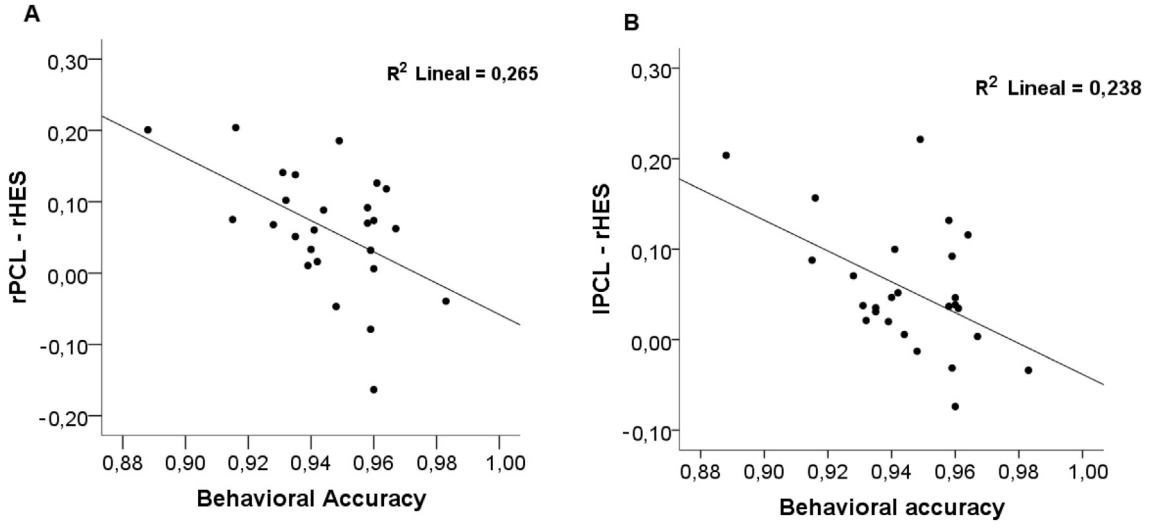

Fig. 7. Significant relationship between connectivity values and behavioral accuracy for: **(A)** Delta band, and **(B)** Theta bands. Each black dot in the plot represents a subject.

during the cue-to-target interval (Shi et al., 2014). Specifically, the connection between the pars opercularis and the parietal cortex is usually involved in the updating of general task representations and might provide relevant stimulus-response associations needed to execute the switching task (Brass and Von Cramon, 2004).

Interestingly, an increased in delta connectivity 600–700 msec post-switch cue, showed that most of the regions found in this time period were connected to the right inferior parietal lobule. This region is known to play an important role as a part of the fronto-parietal network, maintaining task and context information. Further, Keil et al. (2016) suggest that this region may be involved in facilitating stimulus processing. In this case, the connections with the parietal cortex may indicate an exogenously driven and cognitively demanding mental activity (Cocchi et al., 2013). Also, frontal regions and the cingulate cortex synchronized with the inferior parietal cortex suggest that the two systems (fronto-parietal and cingulo-opercular systems) are involved in cognitive control (Dosenbach et al., 2008). Specifically, the fronto-parietal system supposedly processes cue-based information and rapidly implements adaptive control, initiating and adjusting control and maintaining task-relevant information across trials (Cocchi et al., 2013). This network seems to combine brain regions that initiate attentional control at cue onset with regions that process performance feedback to adjust control settings on a trial-by-trial basis (Dosenbach et al., 2008). In contrast, the cingulo-opercular system facilitates maintenance of task-related goals across trials (Cocchi et al., 2013).

Overall, the connectivity profile obtained in this study includes many links involved in these two systems supporting the idea that some functions associated with cognitive control are partly implemented by both systems. In addition, the connections with the inferior parietal lobe from 600 to 700 msec post-cue may be seen as a bridge with other systems such as the hippocampus and the dorsal attention systems, supporting cognitive demands across many task domains. Vincent et al. (2008) found a correlation between the hippocampus, the posterior inferior parietal lobule and the lateral temporal cortex, regions that are also involved in memory processes. Although the fronto-parietal system is not likely to support specific long-term memory functions, this system is known to increase its activity during many working memory and decision-making tasks in addition to memory-retrieval tasks. Specifically, Johnson et al. (2017) found that this fronto-parietal network was also involved in working memory, which was severely impaired in patients with brain lesions in these particular areas. The fronto-parietal control network is therefore anatomically positioned to integrate information from these two opposing brain systems (Vincent et al., 2008). In addition, within 600–700 msec post-cue we found an increase in delta connectivity for the switch cue condition between the left superior parietal cortex and the right supramarginal cortex. These regions, especially the superior parietal cortex, increase their activity when a difficult task is being performed (Crone et al., 2006). Previous evidence suggests that the superior parietal cortex is a common locus both for switching spatial attention and for switching between abstract task rules (Chiu and Yantis, 2009).

During the last time window (700–800 msec), the inferior temporal and occipital cortex increased their delta connectivity in the switch condition. This increment might reflect top-down attention on stimulus attributes when S-R mappings needed to be switched (Stelzel et al., 2011). However, we also obtained higher delta connectivity values in repeat-cue than in switch-cue conditions in all time windows analyzed, mainly between occipitotemporal cortex and limbic regions. Thus, in the repeat cue, we found an increase in connectivity between occipito-temporal regions within 500–600 msec and 600–700 msec post-cue onset. It has been described that some areas within the occipital cortex (as the fusiform gyrus) respond transiently to visual cues, probably reflecting the sensory analysis of the cue. In turn, those areas situated in the posterior parietal cortex, the parietal cortex, and the frontal cortex usually show a more sustained response (Corbetta and Shulman, 2002). In fact, prolonged practice of a task normally produces an increase in neural activity and its duration, even when it is no longer required, an effect probably related to task-inertia (Wylie et al., 2006). Yeung (2006) suggests that task-set inertia affects the occipitotemporal and prefrontal cortices reflecting a similar increase in delta connectivity to repeat cues as the one observed here. Relatedly, within the 500–600 msec and 700–800 msec time windows there was an increase in delta connectivity between posterior cingulate cortex and the temporal cortex. It is known that limbic regions such as the posterior cingulate cortex are involved in maintaining task-set information across trials, and increased delta connectivity may be necessary when repeating an action during the execution of a task (Cocchi et al., 2013).

Additionally, we explored the differences between switch and repeat cues in the theta band. Most task-switching studies associate this frequency band with set switching and proactive control processes (Cooper et al., 2015; Keil et al., 2016). For the switch cue condition, we obtained higher frontoparietal, fronto-temporal and fronto-occipital theta connectivity in the three time windows analyzed. We observed an increase in theta connectivity from 500 to 600 msec in right parsopercularis and right supramarginal gyrus. These regions belong to the fronto-parietal network, which is usually involved in cognitive control. Besides parsopercularis, that is located in the inferior frontal cortex, is involved in maintaining task-relevant information needed for the control of behavior (Yeung, 2006). In addition, during this period, it was found an increase in connectivity between the left entorhinal cortex and left middle frontal gyrus. The connection between these two regions may suggest underlying cognitive processes related with memory and executive function. Recent studies report that these areas are related with high-level cognitive processes, such as memory encoding and retrieval, working memory retention, novelty detection, and top-down control (Cavanagh and Frank, 2014). Additionally, frontotemporal connections, and in particular the medial temporal cortex, have been involved in the coordination of attentional processes to respond to non-expected stimuli (Harper et al., 2017).

From 600 to 700 msec post-switch cue, there was an increase of theta connectivity between right inferior parietal cortex and right posterior cingulate cortex. These two regions are associated with top-down processes related to cognitive control. In recent studies, the posterior cingulate cortex is an important hub that facilitates task-based integration of information between nodes (i.e. anterior cingulate cortex, prefrontal cortex and parietal cortices). Therefore, the posterior cingulate cortex seems to play a key role in managing the coordinated activity of specialized systems to achieve an efficient cognitive control (Cocchi et al., 2013). Additionally, in this time window, the increase of connectivity between the inferior frontal and the superior temporal cortex may indicate memory related processes and also context updating for the next stimulus (Backus et al., 2016; Harper et al., 2017). For the repeat cue, results were similar to those obtained in the delta band. Thus, from 500 to 600 msec, there was an increase in connectivity between inferior frontal and superior temporal cortices. The inferior frontal cortex in connection with the temporal cortex has been implicated in cognitive control processes, guiding the access to relevant information of semantic memory (Badre and Wagner, 2007). Finally, we obtained higher connectivity results between left fusiform and left supramarginal gyrus from 600 to 700 msec for the repeat cue compared to the switch one. These findings suggest that when repeating a rule of action, it is also required an interaction between regions related with both cognitive control and the perceptual analysis of the cue.

A stepwise regression analysis examined which of the significant connectivity differences between cues (if any) were predictive of behavioral efficiency in the switch task. We obtained two significant links for each frequency band that explained a very reasonable percentage of task accuracy (between 20% and 34% depending on the model). For both frequency bands, these links included frontal and temporal brain areas, being the link between the paracentral lobule and superior temporal gyrus the one common structure that explained the largest proportion of

variance in behavioral accuracy. These results (supported by those shown in Fig. 7) highlight that both delta and theta bands jointly help to synchronize similar brain networks to carry out a successful behavior that requires cognitive flexibility (McLelland and VanRullen, 2016), and that the complex time dynamics of cognitive control are best explained by neural oscillations across several frequency bands (cf., Cooper et al., 2016).

The present functional connectivity analyses in the delta and theta bands targeted the latency of the LPC elicited proactively by task cues in task-switching paradigms (Barceló and Cooper, 2018; Rushworth et al., 2002), which has been shown to be largely locked to neither the stimulus nor the response (Brydges and Barceló, 2018). This type of non-phase locked oscillatory long-range synchronization between frontal and temporo-parietal cortices has been proposed to index the type of sensorimotor decision processes necessary for the proactive memory updating of task-set representations at cue onset (Cohen and Donner, 2013). Further, it has also been suggested that non-phase locked power modulations may be more closely linked to cognitive control and to its effects on behavior than the phase-locked event-related potentials reactively elicited by the stimulus itself (Barceló and Cooper, 2018; Cohen and Donner, 2013).

There are some limitations in our attempt to map low frequency EEG phase synchronization patterns with proactive control of action rules in task switching. Firstly, the limitations of conventional F statistics for a correlational study analyzing multiple and highly correlated brain and behavioral measures with small sample sizes; in these cases the use of Bayesian statistics would be more appropriate for testing hypotheses with evidence gathered from small sample sizes (Friston et al., 2002; Wagenmakers, 2007). Second, previous research has shown that increased slow-delta phase coherence over frontotemporal cortical regions is related to temporal expectations of an upcoming imperative stimulus, as delta band phase locking increases with increasing probability of stimulus occurrence (Stefanics et al., 2010). However, since we employed a fixed cue-target interval, the potential confound between temporal predictability and proactive control of task switching cannot be easily discerned with the present task design. Future research making use of different cue-target durations should be able to disentangle the contributions of these two neural processes to the observed effects.

There are also two technical issues regarding the estimation of phase synchronization (PS) indices that merit further discussion. The first one is the well-known issue that zero-lag synchronization can be due to the linear mixing of different sources in two signals. While the source reconstruction procedure helps to deal with this problem, the insufficient spatial resolution of the EEG gives rise to source leakage, a problem whereby the activity of one source "leaks" to the neighboring ones. Various indices of phase synchronization, which are insensitive to zero lag, have been described in the literature (see Bruña et al. (2018) for a recent survey of these methods). However, a recent study suggests (Palva et al., 2018) that these methods may not be sufficient, and that more sophisticated methods are needed to tackle this issue (Ossadtchi et al., 2018; Wang et al., 2018). Therefore, the results presented here correspond to patterns of functional connectivity that should be interpreted in light of these recent works.

The second issue is that, as it has been recently pointed out (Cole et al., 2017; Lozano-Soldevilla et al., 2016), waveforms may not be sinusoidal, which might be presumed to affect the estimation of PS. Yet, even if the waveform is not strictly sinusoidal, the use of a Hilbert transform, which is not affected by the possible non-stationarity in the data, allows estimating PS using ITPC. Indeed the original derivation of the PS concept (Rosenblum et al., 1996) is demonstrated in chaotic systems (in that case, two Rössler systems), whose waveforms are also not sinusoidal. As indicated in this seminal work, the method can be applied to noisy oscillators as well, in which the amplitudes vary along each oscillatory cycle in a different, random way, provided that the signal is periodic, which is guaranteed by the filtering process.

Overall, we conclude that the present study identifies and provides important evidence on the EEG substrates underlying the cued task-switching paradigm. This work confirms and supports the role of delta and theta oscillations in fronto-parietal and cingulo-opercular networks during top-down cognitive control and working memory (Cocchi et al., 2013; Dosenbach et al., 2008; Ekstrom and Watrous, 2014; Vincent et al., 2008). Recent technical advances in functional neuroimaging, such as brain connectivity, allow a refined characterization of large-scale brain system dynamics during cognitive control.

Declarations of interest

None.

Author contributions

M.E.L. and S.P. analyzed the data, prepared all figures, and wrote the main manuscript text. E.P. and F.M. supervised data analyses and wrote the manuscript. F.B. conceived and supervised the project, designed the experimental paradigm, and edited the manuscript. All authors read and approved the final manuscript.

Acknowledgments

Supported by grants from the Fundació la Marató de TV3 (112710) and Spanish Ministry of Economy and Competitiveness (MINECO PSI2013-44760-R) to FB. E. Pereda is supported by MINECO grant (TEC2012-38453-C04-03); ME López by a postdoctoral fellowship from the Spanish Ministry of Economy and Competitiveness (IJCI-2016-30662) and Sandra Pusil by a postdoctoral fellowship from the Spanish Ministry of Economy and Competitiveness (BES-2014-069501).

Appendix A. Supplementary data

Supplementary data to this article can be found online at https://doi.org/10.1016/j.neuroimage.2018.10.068.

References

Adrover-Roig, D., Barceló, F., 2010. Individual differences in aging and cognitive control modulate the neural indexes of context updating and maintenance during task switching. Cortex 46, 434–450. https://doi.org/10.1016/j.cortex.2009.09.012.

Backus, A.R., Schoffelen, J.M., Szebényi, S., Hanslmayr, S., Doeller, C.F., 2016. Hippocampal-prefrontal theta oscillations support memory integration. Curr. Biol. 26, 450–457. https://doi.org/10.1016/j.cub.2015.12.048.

Badre, D., Wagner, A.D., 2007. Left ventrolateral prefrontal cortex and the cognitive control of memory. Neuropsychologia 45, 2883–2901. https://doi.org/10.1016/j.neuropsychologia.2007.06.015.

Barceló, F., 2003. The Madrid card sorting test (MCST): a task switching paradigm to study executive attention with event-related potentials. Brain Res. Protoc. 11, 27–37. https://doi.org/10.1016/S1385-299X(03)00013-8.

Barceló, F., Cooper, P.S., 2018. An information theory account of late frontoparietal ERP positivities in cognitive control. Psychophysiology 55, e12814. https://doi.org/10.1111/psyp.12814.

Bell, A.J., Sejnowski, T.J., 1995. An information-maximization approach to blind separation and blind deconvolution. Neural Comput. 7, 1129–1159.

Benton, A.L., Hamsher, K., 1976. Controlled Oral Word Association Test – COWAT.

Bola, M., Sabel, B.A., 2015. Dynamic reorganization of brain functional networks during cognition. Neuroimage 114, 398–413. https://doi.org/10.1016/j.neuroimage.2015.03.057.

Brass, M., Von Cramon, D.Y., 2004. Decomposing components of task preparation with functional magnetic resonance imaging. J. Cognit. Neurosci. 16, 609–620. https://doi.org/10.1162/089892904323057335.

Braver, T.S., 2012. The variable nature of cognitive control: a dual-mechanisms framework. Trends Cognit. Sci. 16, 106–113. https://doi.org/10.1016/j.tics.2011.12.010.

Braver, T.S., Braver, T.S., Reynolds, J.R., Reynolds, J.R., Donaldson, D.I., Donaldson, D.I., 2003. Neural mechanisms of transient and sustained cognitive control during task switching. Neuron 39, 713–726. https://doi.org/10.1016/S0896-6273(03)00466-5.

Bruña, R., Maestú, F., Pereda, E., 2018. Phase locking value revisited: teaching new tricks to an old dog. J. Neural. Eng. 15, 056011. https://doi.org/10.1088/1741-2552/aacfe4.

Brydges, C.R., Barceló, F., 2018. Functional dissociation of latency-variable, stimulus- and response-locked target P3 sub-components in task-switching. Front. Hum. Neurosci. 12, 60. https://doi.org/10.3389/fnhum.2018.00060.

Cavanagh, J.F., Cohen, M.X., Allen, J.J.B., 2009. Prelude to and resolution of an error: EEG phase synchrony reveals cognitive control dynamics during action monitoring. J. Neurosci. 29, 98–105. https://doi.org/10.1523/JNEUROSCI.4137-08.2009.

Cavanagh, J.F., Frank, M.J., 2014. Frontal theta as a mechanism for cognitive control. Trends Cognit. Sci. 18, 414–421. https://doi.org/10.1016/j.tics.2014.04.012.

Chiu, Y.-C., Yantis, S., 2009. A domain-independent source of cognitive control for task sets: shifting spatial attention and switching categorization rules. J. Neurosci. 29, 3930–3938. https://doi.org/10.1523/JNEUROSCI.5737-08.2009.

Cocchi, L., Zalesky, A., Fornito, A., Mattingley, J.B., 2013. Dynamic cooperation and competition between brain systems during cognitive control. Trends Cognit. Sci. 17, 493–501. https://doi.org/10.1016/j.tics.2013.08.006.

Cohen, M.X., Donner, T.H., 2013. Midfrontal conflict-related theta-band power reflects neural oscillations that predict behavior. J. Neurophysiol. 110, 2752–2763. https://doi.org/10.1152/jn.00479.2013.

Cole, M.W., Reynolds, J.R., Power, J.D., Repovs, G., Anticevic, a, Braver, T.S., 2013. Multi-task connectivity reveals flexible hubs for adaptive task control. Nat. Neurosci. 16, 1348–1355. https://doi.org/10.1038/nn.3470.

Cole, M.W., Schneider, W., 2007. The cognitive control network: integrated cortical regions with dissociable functions. Neuroimage 37, 343–360. https://doi.org/10.1016/j.neuroimage.2007.03.071.

Cole, S.R., van der Meij, R., Peterson, E.J., de Hemptinne, C., Starr, P.A., Voytek, B., 2017. Nonsinusoidal beta oscillations reflect cortical pathophysiology in Parkinson's disease. J. Neurosci. 37, 4830–4840. https://doi.org/10.1523/JNEUROSCI.2208-16.2017.

Cooper, P.S., Darriba, Á., Karayanidis, F., Barceló, F., 2016. Contextually sensitive power changes across multiple frequency bands underpin cognitive control. Neuroimage 132, 499–511. https://doi.org/10.1016/j.neuroimage.2016.03.010.

Cooper, P.S., Wong, A.S.W., Fulham, W.R., Thienel, R., Mansfield, E., Michie, P.T., Karayanidis, F., 2015. Theta frontoparietal connectivity associated with proactive and reactive cognitive control processes. Neuroimage 108, 354–363. https://doi.org/10.1016/j.neuroimage.2014.12.028.

Corbetta, M., Shulman, G.L., 2002. Control of goal-directed and stimulus-driven attention in the brain. Nat. Rev. Neurosci. 3, 215–229. https://doi.org/10.1038/nrn755.

Crone, E.A., Bunge, S.A., Van Der Molen, M.W., Richard Ridderinkhof, K., 2006. Switching between tasks and responses: a developmental study. Dev. Sci. 9, 278–287. https://doi.org/10.1111/j.1467-7687.2006.00490.x.

Desikan, R.S., Ségonne, F., Fischl, B., Quinn, B.T., Dickerson, B.C., Blacker, D., Buckner, R.L., Dale, A.M., Maguire, R.P., Hyman, B.T., Albert, M.S., Killiany, R.J., 2006. An automated labeling system for subdividing the human cerebral cortex on MRI scans into gyral based regions of interest. Neuroimage 31, 968–980.

Dosenbach, N.U.F., Fair, D. a., Cohen, A.L., Schlaggar, B.L., Petersen, S.E., 2008. A dual-networks architecture of top-down control. Trends Cognit. Sci. 12, 99–105. https://doi.org/10.1016/j.tics.2008.01.001.

Dreher, J.-C., Berman, K.F., 2002. Fractionating the neural substrate of cognitive control processes. Proc. Natl. Acad. Sci. U. S. A 99, 14595–14600. https://doi.org/10.1073/pnas.222193299.

Ekstrom, A.D., Watrous, A.J., 2014. Multifaceted roles for low-frequency oscillations in bottom-up and top-down processing during navigation and memory. Neuroimage 85, 667–677. https://doi.org/10.1016/j.neuroimage.2013.06.049.

Friston, K.J., Glaser, D.E., Henson, R.N.A., Kiebel, S., Phillips, C., Ashburner, J., 2002. Classical and bayesian inference in neuroimaging: applications. Neuroimage 16, 484–512. https://doi.org/10.1006/nimg.2002.1091.

Gladwin, T., Lindsen, J., Jong, R. de, 2006. Pre-stimulus EEG effects related to response speed, task switching and upcoming response hand. Biol. Psychol. 72 (1), 15–34. https://doi.org/10.1016/j.biopsycho.2005.05.005.

Gramfort, A., Papadopoulo, T., Olivi, E., Clerc, M., 2010. OpenMEEG: opensource software for quasistatic bioelectromagnetics. Biomed. Eng. Online 9, 45. https://doi.org/10.1186/1475-925X-9-45.

Grange, J., Houghton, G., 2014. Task Switching and Cognitive Control. Oxford University Press, Oxford.

Gulbinaite, R., van Rijn, H., Cohen, M.X., 2014. Fronto-parietal network oscillations reveal relationship between working memory capacity and cognitive control. Front. Hum. Neurosci. 8, 761. https://doi.org/10.3389/fnhum.2014.00761.

Harmony, T., Fernández, T., Silva, J., Bernal, J., Díaz-Comas, L., Reyes, A., Marosi, E., Rodríguez, M., Rodríguez, M., 1996. EEG delta activity: an indicator of attention to internal processing during performance of mental tasks. Int. J. Psychophysiol. 24, 161–171. https://doi.org/10.1016/S0167-8760(96)00053-0.

Harper, J., Malone, S.M., Iacono, W.G., 2017. Theta- and delta-band EEG network dynamics during a novelty oddball task. Psychophysiology 54, 1590–1605. https://doi.org/10.1111/psyp.12906.

Hassan, M., Dufor, O., Merlet, I., Berrou, C., Wendling, F., 2014. EEG source connectivity analysis: from dense array recordings to brain networks. PloS One 9, e105041. https://doi.org/10.1371/journal.pone.0105041.

Jensen, A.R., Rohwer, W.D., 1966. The Stroop color-word test: a review. Acta Psychol. 25, 36–93.

Johnson, E.L., Dewar, C.D., Solbakk, A.K., Endestad, T., Meling, T.R., Knight, R.T., 2017. Bidirectional frontoparietal oscillatory systems support working memory. Curr. Biol. 27, 1829–1835 e4. https://doi.org/10.1016/j.cub.2017.05.046.

Keil, J., Pomper, U., Senkowski, D., 2016. Distinct patterns of local oscillatory activity and functional connectivity underlie intersensory attention and temporal prediction. Cortex 74, 277–288. https://doi.org/10.1016/j.cortex.2015.10.023.

Kiesel, A., Steinhauser, M., Wendt, M., Falkenstein, M., Jost, K., Philipp, A.M., Koch, I., 2010. Control and interference in task switching–a review. Psychol. Bull. 136, 849–874. https://doi.org/10.1037/a0019842.

Lachaux, J.P., Rodriguez, E., Martinerie, J., Varela, F.J., 1999. Measuring phase synchrony in brain signals. Hum. Brain Mapp. 8, 194–208.

Le, T., Pardo, J., Hu, X., 1998. 4 T-fMRI study of nonspatial shifting of selective attention: cerebellar and parietal contributions. J. Neurophysiol. 79 (3), 1535–1548. https://doi.org/10.1152/jn.1998.79.3.1535.

Lozano-Soldevilla, D., Ter Huurne, N., Oostenveld, R., 2016. Neuronal oscillations with non-sinusoidal morphology produce spurious phase-to-amplitude coupling and directionality. Front. Comput. Neurosci. 10, 87. https://doi.org/10.3389/fncom.2016.00087.

Mansfield, E., Karayanidis, F., 2012. Switch-related and general preparation processes in task-switching: evidence from multivariate pattern classification of eeg data. J. Neurosci. 12–32 (50), 18253–18258. https://doi.org/10.1523/JNEUROSCI.0737-12.2012.

Maris, E., Oostenveld, R., 2007. Nonparametric statistical testing of EEG- and MEG-data. J. Neurosci. Methods 164, 177–190. https://doi.org/10.1016/j.jneumeth.2007.03.024.

McLelland, D., VanRullen, R., 2016. Theta-gamma coding meets communication-through-coherence: neuronal oscillatory multiplexing theories reconciled. PLoS Comput. Biol. 12, e1005162. https://doi.org/10.1371/journal.pcbi.1005162.

Monsell, S., 2003. Task switching. Trends Cognit. Sci. 7, 134–140.

Mosher, J.C., Baillet, S., Leahy, R.M., 2003. Equivalence of linear approaches in bioelectromagnetic inverse solutions. In: IEEE Workshop on Statistical Signal Processing, 2003. IEEE, pp. 294–297. https://doi.org/10.1109/SSP.2003.1289402.

Ossadtchi, A., Altukhov, D., Jerbi, K., 2018. Phase shift invariant imaging of coherent sources (PSIICOS) from MEG data. Neuroimage S1053–8119 (18), 30731–30736. https://doi.org/10.1016/j.neuroimage.2018.08.031.

Palva, J.M., Wang, S.H., Palva, S., Zhigalov, A., Monto, S., Brookes, M.J., Schoffelen, J.-M., Jerbi, K., 2018. Ghost interactions in MEG/EEG source space: a note of caution on inter-areal coupling measures. Neuroimage 173, 632–643. https://doi.org/10.1016/j.neuroimage.2018.02.032.

Palva, S., Palva, J.M., 2012. Discovering oscillatory interaction networks with M/EEG: challenges and breakthroughs. Trends Cognit. Sci. 16, 219–230. https://doi.org/10.1016/j.tics.2012.02.004.

Power, J.D., Petersen, S.E., 2013. Control-related systems in the human brain. Curr. Opin. Neurobiol. 23, 223–228. https://doi.org/10.1016/j.conb.2012.12.009.

Raghavachari, S., Lisman, J., Tully, M., 2006. Theta oscillations in human cortex during a working-memory task: evidence for local generators. J. Neurophysiol. 95 (3), 1630–1638. https://doi.org/10.1152/jn.00409.2005.

Rogers, R.D., Monsell, S., 1995. Costs of a predictible switch between simple cognitive tasks. J. Exp. Psychol. Gen. 124, 207–231. https://doi.org/10.1037/0096-3445.124.2.207.

Rosenblum, M.G., Pikovsky, A.S., Kurths, J., 1996. Phase synchronization of chaotic oscillators. Phys. Rev. Lett. 76, 1804–1807. https://doi.org/10.1103/PhysRevLett.76.1804.

Rousselet, G.A., Foxe, J.J., Bolam, J.P., 2016. A few simple steps to improve the description of group results in neuroscience. Eur. J. Neurosci. 44, 2647–2651. https://doi.org/10.1111/ejn.13400.

Rushworth, M.F.S., Passingham, R.E., Nobre, A.C., 2002. Components of switching intentional set. J. Cognit. Neurosci. 14, 1139–1150. https://doi.org/10.1162/089892902760807159.

Sauseng, P., Griesmayr, B., Freunberger, R., 2010. Control mechanisms in working memory: a possible function of EEG theta oscillations. BioBehav. Rev. 34 (7), 1015–1022. https://doi.org/10.1016/j.neubiorev.2009.12.006.

Sauseng, P., Hoppe, J., Klimesch, W., Gerloff, C., Hummel, F.C., 2007. Dissociation of sustained attention from central executive functions: local activity and interregional connectivity in the theta range. Eur. J. Neurosci. 25, 587–593. https://doi.org/10.1111/j.1460-9568.2006.05286.x.

Shi, Y., Meindl, T., Szameitat, A.J., Müller, H.J., Schubert, T., 2014. Task preparation and neural activation in stimulus-specific brain regions: an fMRI study with the cued task-switching paradigm. Brain Cognit. 87, 39–51. https://doi.org/10.1016/j.bandc.2014.03.001.

Simpson, G., Weber, D., Dale, C., 2011. Dynamic activation of frontal, parietal, and sensory regions underlying anticipatory visual spatial attention. J. Neurosci. 28–31 (39), 13880–13889. https://doi.org/10.1523/JNEUROSCI.1519-10.2011.

Sporns, O., Chialvo, D., Kaiser, M., Hilgetag, C., 2004. Organization, development and function of complex brain networks. Trends Cogn 8 (9), 418–425. https://doi.org/10.1016/j.tics.2004.07.008.

Stefanics, G., Hangya, B., Hernádi, I., Winkler, I., Lakatos, P., Ulbert, I., 2010. Phase entrainment of human delta oscillations can mediate the effects of expectation on reaction speed. J. Neurosci. 30, 13578–13585. https://doi.org/10.1523/JNEUROSCI.0703-10.2010.

Stelzel, C., Basten, U., Fiebach, C.J., 2011. Functional connectivity separates switching operations in the posterior lateral frontal cortex. J. Cognit. Neurosci. 23, 3529–3539. https://doi.org/10.1162/jocn_a_00062.

Tadel, F., Baillet, S., Mosher, J.C., Pantazis, D., Leahy, R.M., 2011. Brainstorm: a user-friendly application for MEG/EEG analysis. Comput. Intell. Neurosci. 2011. https://doi.org/10.1155/2011/879716.

Toth, L., Assad, J., 2002. Dynamic coding of behaviourally relevant stimuli in parietal cortex. Nature 10–415 (6868), 165–168. https://doi.org/10.1038/415165a.

Vandierendonck, A., Liefooghe, B., 2010. Task switching: interplay of reconfiguration and interference control. Psychol. Bull. 136 (4), 601–626. https://doi.org/10.1037/a0019791.

Vincent, J.L., Kahn, I., Snyder, A.Z., Raichle, M.E., Buckner, R.L., 2008. Evidence for a frontoparietal control system revealed by intrinsic functional connectivity. J. Neurophysiol. 100, 3328–3342. https://doi.org/10.1152/jn.90355.2008.

Wagenmakers, E.-J., 2007. A practical solution to the pervasive problems ofp values. Psychon. Bull. Rev. 14, 779–804. https://doi.org/10.3758/BF03194105.

Wang, L., Liu, X., Guise, K.G., Knight, R.T., Ghajar, J., Fan, J., 2010. Effective connectivity of the fronto-parietal network during attentional control. J. Cognit. Neurosci. 22, 543–553. https://doi.org/10.1162/jocn.2009.21210.

Wang, S.H., Lobier, M., Siebenhühner, F., Puoliväli, T., Palva, S., Palva, J.M., 2018. Hyperedge bundling: data, source code, and precautions to modeling-accuracy bias to synchrony estimates. Data Br 18, 262–275. https://doi.org/10.1016/j.dib.2018.03.017.

Wechsler, D., 2008. Wechsler Adult Intelligence Scale—fourth Edition Administration and Scoring Manual. San Antonio, TX: Pearson.

Wylie, G.R., Javitt, D.C., Foxe, J.J., 2006. Jumping the gun: is effective preparation contingent upon anticipatory activation in task-relevant neural circuitry? Cereb. Cortex 16, 394–404. https://doi.org/10.1093/cercor/bhi118.

Yekutieli, D., Benjamini, Y., 2001. He control of the false discovery rate in multiple testing under dependency. Ann. Stat. 29, 1165–1188. https://doi.org/10.1214/aos/1013699998.

Yeung, N., 2006. Between-task competition and cognitive control in task switching. J. Neurosci. 26, 1429–1438. https://doi.org/10.1523/JNEUROSCI.3109-05.2006.

Zanto, T.P., Rubens, M.T., Bollinger, J., Gazzaley, A., 2010. Top-down modulation of visual feature processing: the role of the inferior frontal junction. Neuroimage 53, 736–745. https://doi.org/10.1016/j.neuroimage.2010.06.012.

Zanto, T.P., Rubens, M.T., Thangavel, A., Gazzaley, A., 2011. Causal role of the prefrontal cortex in top-down modulation of visual processing and working memory. Nat. Neurosci. 14, 656–661. https://doi.org/10.1038/nn.2773.